Journal of ELECTRICAL ENGINEERING, VOL 73(2022), NO1, 36–42

sciendo

PAPERS

Frequency diverse array radar with non-uniform array spacing based on sigmoid function

Zeeshan Ahmad[1], Zain ul Abidin Jaffri[2*], Shu-Di Bao[1], Meng Chen[1]

As a widely recognized electronic beam steering concept, frequency diverse array (FDA) radar is an effective and feasible solution to provide beam scanning ability in both angle as well as range dimension as a function of time. However, the conventional FDA radar employing progressive incremental frequency offsets across the array elements generates an S-shaped and range-angle coupled beampattern. As such, the FDA beampattern can be decoupled into range-angle dimensions by employing non-linear frequency offsets or using non-uniform arrays. Frequency offsets design has been extensively researched in recent years, whereas non-uniform arrays were given little attention so far. In this paper, we propose a novel FDA radar with a unified configuration of non-uniform linear array, and non-linear frequency offsets to achieve a high-resolution dot-shaped range-angle dependent beampattern. More specifically, the non-uniform inter-element spacing is calculated using the sigmoid function, and non-linear frequency offsets are generated by logistic map, and triangular window function. Simulation results clearly demonstrate the performance advantages of the proposed FDA radar in terms of beam width and side lobe levels.

K e y w o r d s: beampattern synthesis, frequency diverse array, frequency offsets, non-uniform array, triangular window

1 Introduction

Phased array (PA) radars have demonstrated outstanding performance in scanning their beam electronically with high directivity [1–3]. However, the conventional PA radar employs highly expensive phase-shifters at each element to direct a beam in the desired direction [2]. In addition, the resulting beampattern is only angle-dependent. Consequently, PA radars cannot distinguish targets from different ranges in a particular angle in the presence of inherent range ambiguity [3–5]. Recently, a new electronic scanning concept, namely, frequency diverse array (FDA) radar has received noticeable attention due to its unique range-angle dependent beampattern [4]. Unlike conventional PA radars whose transmit elements radiate fixed carrier frequencies, the FDA radar employ a small frequency offset across the array elements to achieve beam steering as a function of angle, range and time [5].

The concept of FDA radar with progressive incremental frequency offsets was first proposed by Antonik *et al* in 2006 [6]. This progressive frequency shift in radiated signals enable the FDA radar to realize rangeangular beamforming and auto-scanning feature without using the expensive phase-shifters [7]. However, the beampattern of a conventional FDA radar is coupled in range and angle dimensions. As such, employing non-uniform array or random frequency offsets can decouple the FDA beampattern into range and angle dimensions [7–9].

Until recently, several attractive functions have been proposed to design suitable frequency offsets, where uniform linear array (ULA) is the most commonly used array configuration. Among the various frequency offset designs, Hamming window based non-uniform frequency offsets [10], logarithmic frequency offsets [11], logistic map based random frequency offsets [12], modified sinusoidal frequency offsets [13], Taylor windowed frequency offsets [14], and others [15–17], are the most popular designs. Beside these fixed frequency offset schemes, FDAs with time-modulated frequency offsets have been proposed in [18–21] to achieve time-invariant range-angle dependent beampatterns. Although FDAs with above-mentioned frequency offset schemes achieve a dot-shaped range-angle decoupled beampattern, their focusing performance is not optimal [22]. In general, these FDAs based on ULA configuration have high sidelobe levels, and poor resolution [23]. In contrast, there are few studies on other array geometries [24]. Several different array configurations such as coprime, sparse, planar, and uniform circular array have also been reported for improved beampattern synthesis [22]. Recently, non-uniformly spaced FDAs is also getting attention [24]. Compared to the ULA configuration, non-uniform arrays have provable performance guarantee in achieving better sidelobe suppression in the literature [23, 24].

In this paper, we present a novel design of a non-uniform FDA radar where the non-uniform inter-element spacing is calculated by using the sigmoid function. Two non-linear frequency offsets schemes based on logistic map, and triangular window function are devised to analyze the proposed FDA radar. The non-linear frequency

[1] School of Electronic and Information Engineering, Ningbo University of Technology, Ningbo 315211, People's Republic of China,
[2] College of Physics and Electronic Information Engineering, Neijiang Normal University Neijiang 641100, People's Republic of China,
* Corresponding author: zainulabidin.jaffri@gmail.com

https://doi.org/10.2478/jee-2022-0005, Print (till 2015) ISSN 1335-3632, On-line ISSN 1339-309X

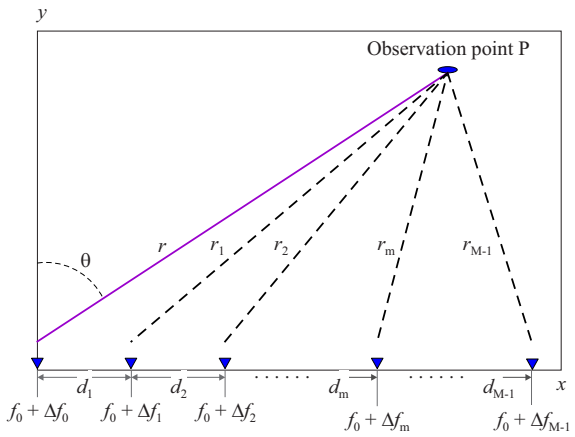

Fig. 1. Proposed non-uniform FDA radar configuration

offsets facilitate to achieve a dot shaped range-angle decoupled beampattern, whereas the non-uniform array is helpful in achieving minimum sidelobe levels and high resolution. It has been shown through simulations that the proposed FDA radar outperforms existing FDAs in terms of sidelobe suppression and mainlobe width.

2 Proposed non-uniform FDA radar

In this section, we first devise two frequency offsets schemes designed by logistic map, and triangular window function, then calculate the inter-element spacing for the non-uniform distribution of the array elements. Finally, the transmit beampattern synthesis of the proposed non-uniform FDA radar is derived.

2.1 Frequency offset

Consider a non-uniform linear array configuration composed of M omni-directional elements as shown in Fig. 1. The inter-element spacing is d_m, where $m = 0, 1, \ldots, M-1$. The frequency of the signal radiated by the m-th element can be expressed as [7];

$$f_m = f_0 + \Delta f_m, \tag{1}$$

where f_0 denotes the reference frequency, and Δf_m is the inter-element frequency offset of the m-th element.

Frequency offsets play a pivotal role in shaping the FDA's beampattern [25]. As discussed previously, progressive incremental frequency offsets yield a time-periodic S-shaped range-angle coupled beampattern, and non-linear frequency offsets generate a dot-shaped aperiodic range-angle dependent beampattern. Here, we propose two non-linear frequency offsets schemes designed by logistic map, and triangular window function to achieve a focused dot-shaped beampattern at the target location.

The proposed non-linear frequency offset based on logistic map is derived as

$$\Delta f_m = (-1)^m g(m) \Delta f\,, \tag{2}$$

where

$$g(m) = \begin{cases} g_0, m = 0, \quad 0 < g_0 < 1 \\ \mu g_{m-1}(1 - g_{m-1}), \quad \mu \in [0, 4]\,, \end{cases} \tag{3}$$

is a non-linear function generated by a logistic map [22], Δf is the coefficient for frequency shift which is far less than the carrier frequency f_0, and the term $(-1)^m$ is used to alternate the values of the frequency offsets across the array elements. For $g(m)$ to remains bounded on

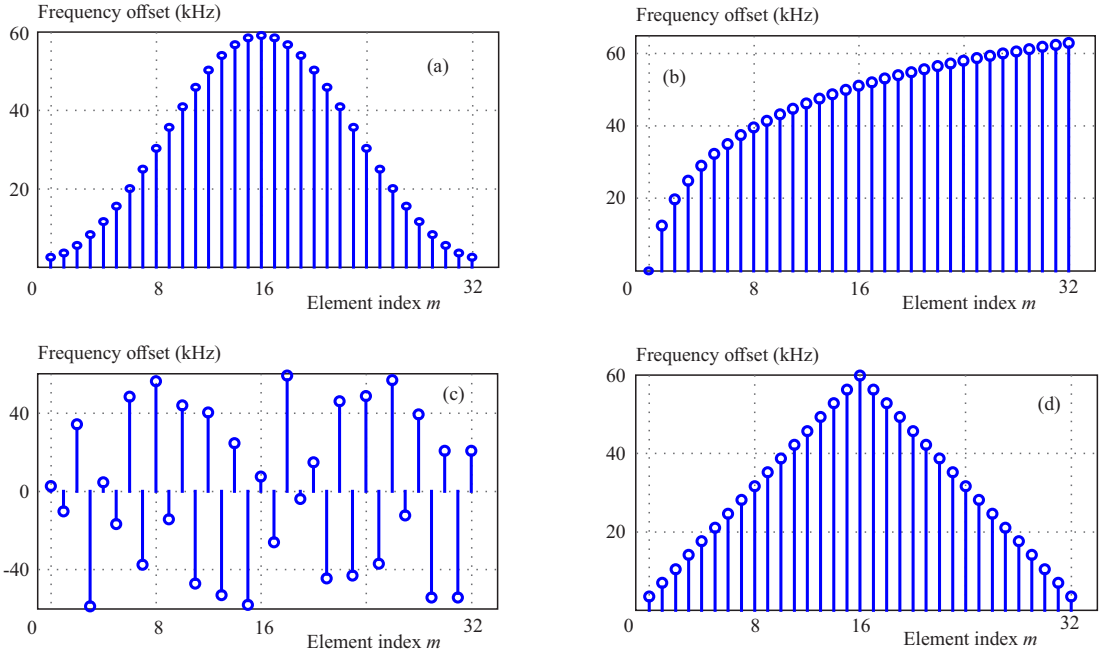

Fig. 2. Comparison of frequency offsets generated by: (a) – Taylor window, (b) – logarithmic, (c) – logistic map, and (d) – triangular window

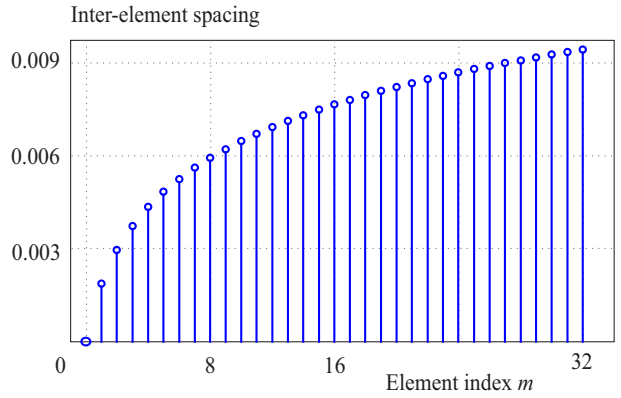

Fig. 3. Inter-element spacing using sigmoid function

$[0, 1]$, the parameter μ should be chosen in the range $[0, 4]$ [7]. With $\mu > 4$, any initial value g_0 will lead the $g(m)$ beyond the interval $[0, 1]$. Similarly, if the initial value g_0 is 0 or 1, all the subsequent values of $g(m)$ would be zero [22].

Window functions are exclusively used for frequency offset generation in FDAs due to their simple implementation [2]. Therefore, we have incorporated the triangular window function to generate non-linear frequency offsets. The non-linear frequency offsets based on the triangular window function is defined as

$$\Delta f_m = h(m)\Delta f\,, \tag{4}$$

where,

$$h(m) = \begin{cases} \frac{2m}{M}, & m = 0, 1, \ldots, \frac{M}{2} - 1 \\ 2 - \frac{2m}{M}, & m = \frac{M}{2}, \ldots, M - 1 \end{cases}, \tag{5}$$

is the triangular window function [30].

The distribution of various frequency offset schemes across the array elements are compared in Fig 2.

The frequency offsets employed in FDAs must satisfy certain conditions. The range-angle dependency of the FDA beampattern is ensured only if $\Delta f_m > 0$. When $\Delta f_m = 0$, the FDA beampattern reduces to only angle-dependent as conventional phased arrays. Similarly, the upper limit on frequency offsets to guarantee a narrow-band system is $\Delta f_m < \frac{f_0}{10}$. In addition to the above-mentioned numerical limits, random frequency offsets

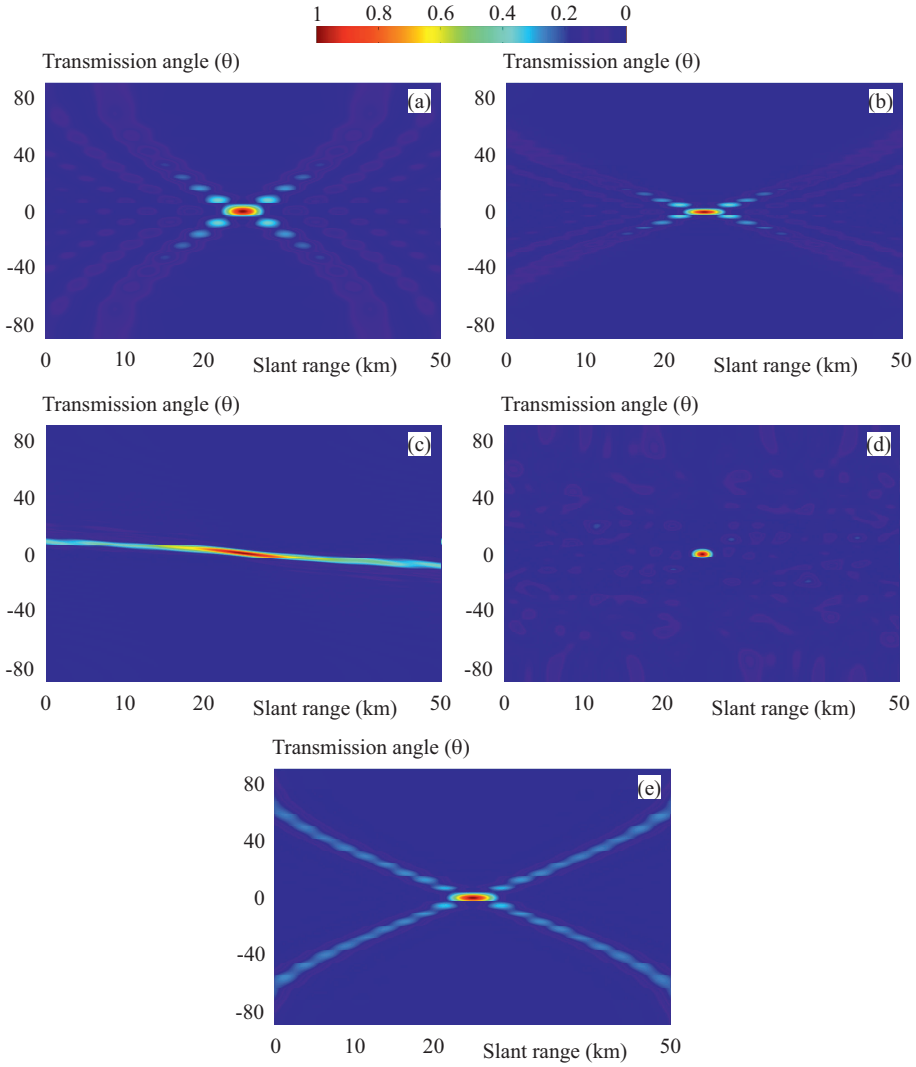

Fig. 4. Beampattern synthesis results: (a) – Hamming FDA, (b) – Taylor FDA, (c) – logarithmic FDA, (d) – logistic NU-FDA, and (e) – triangular NU-FDA

should be employed to realize a beampattern with a single maximum at the target location. The non-uniform frequency offsets alter the synchronization between linear increasing frequency offsets and element spacing to avoid range-angle coupling in the FDA beampattern [7, 22].

2.2 Non-uniform array spacing

Compared to conventional FDA configuration whose elements are uniformly distributed across the array, the inter-element spacing for the proposed non-uniform FDA radar calculated by the sigmoid function [26] is given as

$$f(z) = \frac{e^z}{e^z + 1}. \tag{6}$$

By replacing the term z with $\log(m)$, the non-uniform inter-element spacing for each element can be calculated as;

$$d_m = \begin{cases} d_0 = 0, \quad m = 0 \\ d_m = d\left[\dfrac{e^{\log(m)}}{e^{\log(m)}+1}\right],\ m = 1, 2, \ldots, M-1 \end{cases}, \tag{7}$$

where $d \leq \frac{\lambda}{2}$ is the fundamental inter-element spacing. Here, λ denotes the wavelength. Since the range of sigmoid function is 0 to 1, d in the above equation ensures that the maximum inter-element spacing does not exceed the fundamental element spacing. Moreover, the size of the antenna can also be controlled by the fundamental inter-element spacing. The inter-element spacing for a 33-elements array using sigmoid function with $d = \frac{\lambda}{3}$ is shown in Fig. 3

2.3 Transmit beampattern synthesis

The signal transmitted by the m-th element of the non-uniform FDA radar can be modelled as [1–5];

$$s_m(t) = w_m \exp\{-j2\pi f_m t\}, \quad t \in [0, T], \tag{8}$$

where w_m denotes the complex weight associated with the m-th element, and T represents the transmitted pulse duration. The overall signal arriving at an arbitrary point $P(r, \theta)$ in the far-field can be expressed as [1-9];

$$\begin{aligned} S(t, r, \theta) &= \sum_{m=0}^{M-1} s_m\Big(t - \frac{r_m}{c}\Big) \\ &= \sum_{m=0}^{M-1} w_m \exp\Big\{-j2\pi f_m\Big(t - \frac{r_m}{c}\Big)\Big\}, \end{aligned} \tag{9}$$

where $r_m \cong r - md_m \sin\theta$ is the slant range with respect to the m-th element [22], and c is the speed of light. Substituting $r_m \cong r - md_m \sin\theta$ and (1) into (9), we have [10–15];

$$\begin{aligned} S(t, r, \theta) &= \sum_{m=0}^{M-1} w_m \exp\Big\{-j2\pi(f_0 + \Delta f_m)\Big[t - \frac{r - md_m \sin\theta}{c}\Big]\Big\} \\ &= \exp\{\phi_0\} \sum_{m=0}^{M-1} w_m \exp\Big\{-j2\pi\Big[\Delta f_m\Big(t - \frac{r}{c}\Big) \\ &\quad + \Delta f_m\Big(\frac{md_m \sin\theta}{c}\Big) + f_0\Big(\frac{md_m \sin\theta}{c}\Big)\Big]\Big\}, \end{aligned} \tag{10}$$

where $\Delta f_m \frac{md_m \sin\theta}{c} < \pm\frac{\pi}{4}$ because $\max\{\Delta f_m\} \ll f_0$ [1-3], Hence, the quadratic phase term $\Delta f_m \frac{md_m \sin\theta}{c}$, and $\phi_0 = -j2\pi f_0(t - \frac{r}{c})$ can be discarded in the further analysis [7]. The corresponding array factor is then derived as [1–9];

$$\begin{aligned} AF(t, r, \theta) = \sum_{m=0}^{M-1} w_m \exp\Big\{-j2\pi\Big[\Delta f_m\Big(t - \frac{r}{c}\Big) \\ + f_0\Big(\frac{md_m \sin\theta}{c}\Big)\Big]\Big\}. \end{aligned} \tag{11}$$

The transmit weights to ensure the maximum of the beampattern at the desired target location can be computed as;

$$w_m = \exp\Big\{-j2\pi\Big[\frac{\Delta f_m r_d}{c} - \frac{md_m f_0 \sin\theta_d}{c}\Big]\Big\}. \tag{12}$$

Accordingly, the beampattern towards the desired target location $P(r_d, \theta_d)$ is given as [10–12];

$$\begin{aligned} B(t, r_d, \theta_d) = \Bigg|\sum_{m=0}^{M-1} \exp\Big\{-j2\pi\Big[\Delta f_m\Big(t - \Big(\frac{r - r_d}{c}\Big)\Big) \\ + \Big(\frac{f_0 md_m(\sin\theta - \sin\theta_d)}{c}\Big)\Big]\Big\}\Bigg|^2. \end{aligned} \tag{13}$$

3 Numerical simulations

In this section, we present simulation results that demonstrate the performance improvement achievable through the proposed FDA radar. We evaluate the performance of the proposed FDA radar in comparison to Hamming FDA [10], Log-FDA [11], and Taylor FDA [14]. The simulation parameters for the proposed non-uniform FDA radar are listed in Table 1. For fair comparison, the maximum frequency offset $\Delta f_{\max}$ is set as 60 kHz to ensure the same bandwidth for all the FDAs considered for comparison. The initial value for the logistic map is set to $g_0 = 0.045$, and $\mu = 4$. With $\mu = 4$, sequence of values of Δf_m seems random and chaotic, and initial value g_0 controls the resolution and sidelobes in the beampattern. The initial value can also be adjusted by using some optimization algorithm for better results.

In the first example, we compared the normalized transmit beampatterns in range-angle dimensions. The results are shown in Fig. 4. It is observed from Fig. 4 that all the given FDAs achieve a focused dot-shaped beampattern at the target position. However, the proposed FDA radar with logistic map and triangular window-based frequency offsets has sharper focusing beampattern with compact mainlobe and reduced sidelobes.

Table 1. Simulation parameters

Parameter	Symbol	Value
Reference carrier frequency	f_0	10 GHz
Number of array elements	M	33
Desired target location	$P(r_d, \theta_d)$	(25 km, 0°)
Frequency shift	Δf	60 kHz
Fundamental element spacing	d	0.01 m
Length of antenna array	L	0.294 m

To see more clearly the resolution performance of the proposed non-uniform FDA radar, the normalized profiles of resultant beampatterns are plotted separately in range and angle dimensions in Fig. 5. It is evident that the proposed non-uniform FDA radar using logistic map based frequency offsets and triangular window based frequency offsets significantly outperforms existing FDAs in terms of half-power beamwidth (HPBW) and peak sidelobe level (P-SLL). Moreover, the proposed non-uniform FDA radar with logistic map based frequency offsets is observed to have narrower main beamwidth while the FDA with triangular window based frequency offsets outperforms in sidelobe suppression. On the other hand, the P-SLL in range dimension for the proposed non-uniform FDA radar with logistic map based frequency offsets is slightly higher than that with triangular window based frequency offsets.

Next, we demonstrate the scanning performance of the proposed non-uniform FDA radar. The normalized profile patterns with different ranges and angles for the proposed non-uniform FDA radar employing logistic map based frequency offsets, and triangular window based frequency offsets are given in Fig. 6 and Fig. 7, respectively. From Fig. 6(a),(b) and Fig. 7(a),(b), it is noted that the proposed FDA radar preserve the same main-lobe width and P-SLL at different ranges and angles, which makes it suitable for practical applications.

Finally, the effect of frequency shift coefficient Δf on the performance of the proposed FDA radar is considered. The HPBW and P-SLL curves with respect to different values of Δf are plotted in Fig. 8. From Fig. 8, it can be found that when Δf increases, the HPBWs for both the FDAs get narrow modestly. Moreover, the P-SLL remains the same for all values of the Δf.

Therefore, we can conclude that the performance of the proposed FDA radar has been improved evidently by utilizing non-uniform inter-element spacing and random frequency offsets. Moreover, the proposed non-uniform distribution of array element achieves miniaturization of the antenna [27–29] which is an attractive feature for various next-generation applications. The length of the 33-elements antenna array with proposed non-uniform dis-

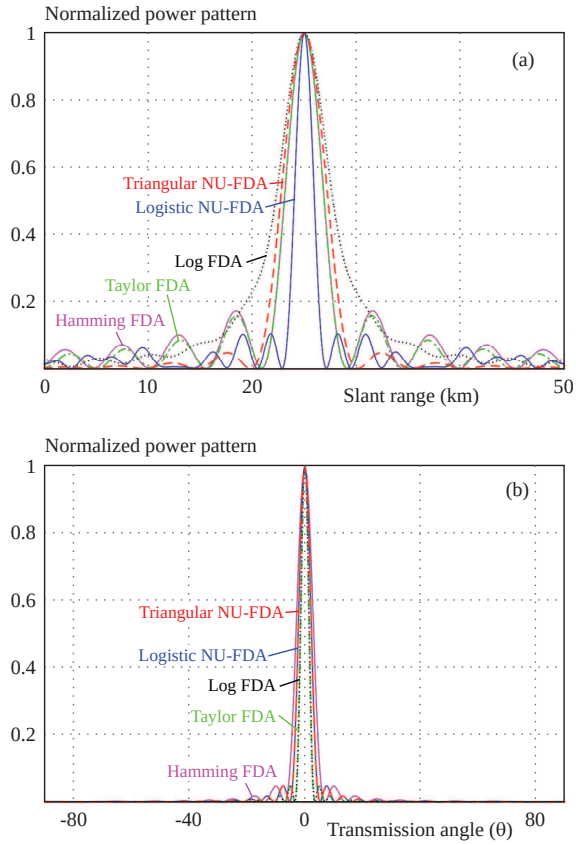

Fig. 5. Normalized beampattern profiles in: (a) – range dimension, (b) – angle dimension

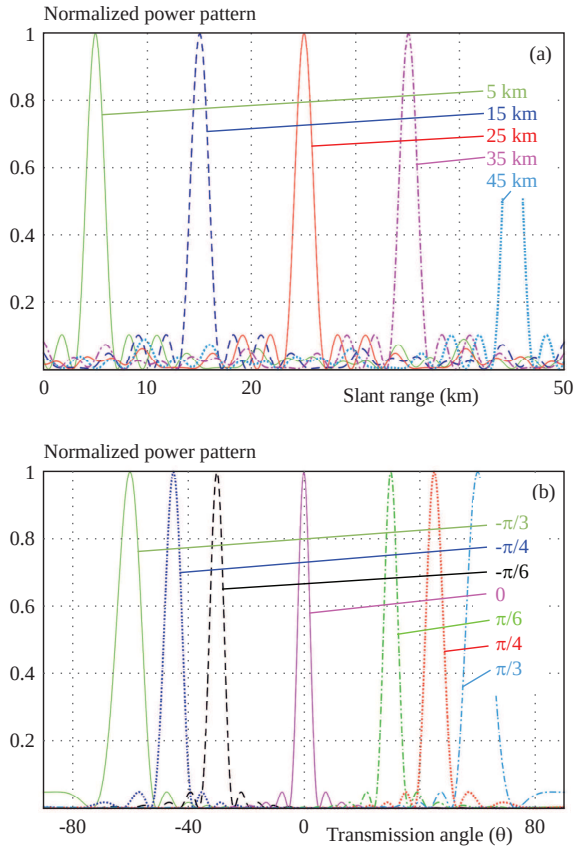

Fig. 6. Scanning performance of the proposed non-uniform FDA radar with logistic map based frequency offsets: (a) – range profile, (b) – angle profile

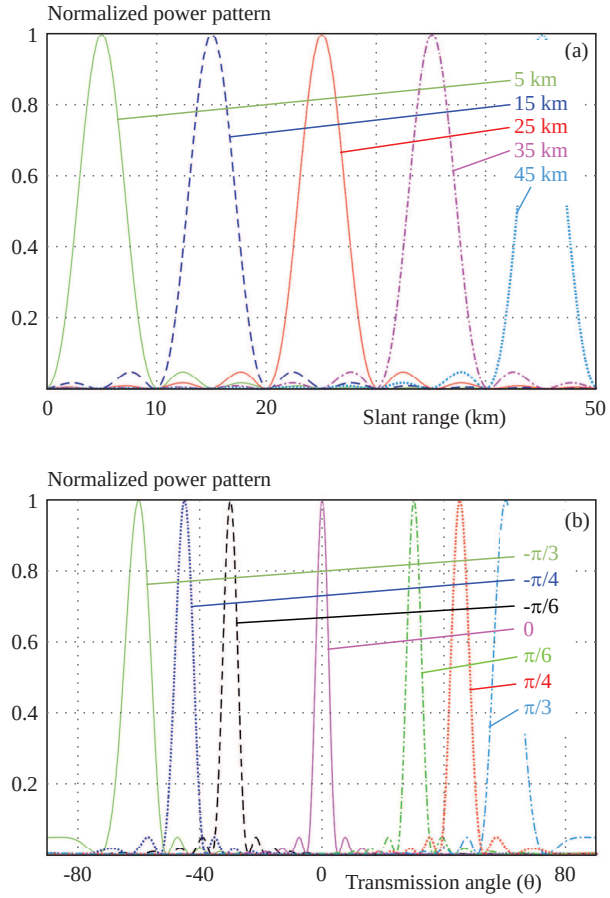

Fig. 7. Scanning performance of the proposed non-uniform FDA radar with triangular window based frequency offsets: (a) – range profile, (b) – angle profile

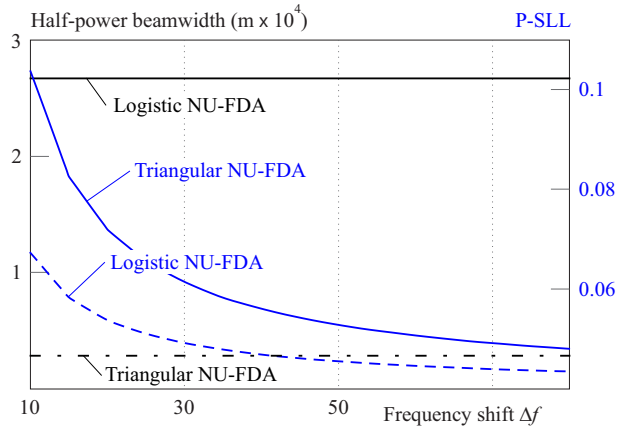

Fig. 8. HPBW and P-SLL versus frequency shift coefficient Δf

tribution is 0.294 m, whereas length of an array with the same number of uniformly spaced elements is 0.480 m.

4 Conclusion

In this paper, we proposed a novel FDA radar with non-uniform inter-element spacing based on the sigmoid function. The proposed non-uniform FDA radar employs non-linear frequency offsets based on logistic map, and triangular window to realize a range-angle decoupled beampattern. Simulation results demonstrate that the proposed non-uniform FDA radar offer significant performance improvement over other existing ULA based FDAs in terms of HPBW and P-SLL.

Acknowledgements

This work was supported in part by the National Natural Science Foundation of China under Grant 61671260.

References

[1] A. Basit, W.-Q. Wang, and S.Y. Nusenu, "Adaptive transmit beamspace design for cognitive FDA radar tracking," *IET Radar, Sonar & Navigation*, vol. 13, no. 12, pp. 2083-2092, 2019.

[2] Z. Ahmad, M. Chen, and S.-D. Bao, "Beampattern analysis of frequency diverse array radar: a review," *EURASIP Journal on Wireless Communications and Networking*, vol. 2021, p. 189, 2021.

[3] A. Basit, W. Khan, S. Khan, and I.M. Qureshi, "Development of frequency diverse array radar technology: a review," *IET Radar, Sonar & Navigation*, vol. 12, no. 2, pp. 165–175, 2018.

[4] H. Zeng, Z. Ahmad, J. Zhou, Q. Wang, and Y. Wang, "DOA estimation algorithm based on adaptive filtering in spatial domain," *China Communications*, vol. 13, no. 12, pp. 49–58, 2016.

[5] A. Basit, W.-Q. Wang, and S.Y. Nusenu, "Adaptive transmit array sidelobe control using FDA-MIMO for tracking in joint radar-communications," *Digital Signal Processing*, vol. 97, p. 102619, 2020.

[6] P. Antonik, M.C. Wicks, H.D. Griffiths, and C.J. Baker,, "Frequency diverse array radars," in*Proceedings of IEEE Radar Conference*, Verona, NY, USA, 2006, pp. 215–217.

[7] Z. Ahmad, Z. Shi, C. Zhou, and Y. Gu, "Time-variant focused range-angle dependent beampattern synthesis by frequency diverse array radar," *IET Signal Processing*, vol. 14, no. 6, pp. 352–360, 2020.

[8] W.-Q. Wang, H.C. So, and H. Shao, "Nonuniform frequency diverse array for range-angle imaging of targets," *IEEE Sensors Journal*, vol. 14, no. 8, pp. 2469–2476, 2014.

[9] C. Cui, W. Li, X. Ye, Y. Hei, and X. Shi, "A short-timerange-angle decoupled beampattern synthesis for frequency diverse arrays", *IET Microwaves & Antennas Propagation*, vol. 15, no. 8, pp. 855–870, 2021.

[10] A. Basit, I. M. Qureshi, W. Khan, S. U. Rehman, and M. M. Khan, "Beam pattern synthesis for an FDA radar with Hamming window-based nonuniform frequency offset," *IEEE Antennas and Wireless Propagation Letters*, vol. 16, pp. 2283–2286, 2017.

[11] W. Khan, I.M. Qureshi, and S. Saeed, "Frequency diverse array radar with logarithmically increasing frequency offset," *IEEE Antennas and Wireless Propagation Letters*, vol. 14, pp. 499–502, 2015.

[12] Z. Wang, T. Mu, Y. Song, and Z. Ahmad, "Beamforming of frequency diverse array radar with nonlinear frequency offset based on logistic map," *Progress in Electromagnetics Research M*, vol. 64, pp. 55–63, 2018.

[13] X. Shao, T. Hu, Z. Xiao and J. Zhang, "Frequency diverse array beampattern synthesis with modified sinusoidal frequency offset," *IEEE Antennas and Wireless Propagation Letters*, vol. 20, no. 9, pp. 1784–1788, 2021.

[14] Y. Liao, H. Tang, X. Chen, and W.-Q. Wang, "Frequency diverse array beampattern synthesis with Taylor windowed frequency offsets," *IEEE Antennas and Wireless Propagation Letters*, vol. 19, no. 11, pp. 1901–1905, 2020.

[15] M. Mahmood and H. Mir, "FDA transmit beampattern synthesis using piecewise trigonometric frequency offset," *IET Radar, Sonar & Navigation*, vol. 13, no. 7, pp. 1149–1153, 2019.

[16] K. Gao, W. Wang, J. Cai, and J. Xiong, "Decoupled frequency diverse array range-angle-dependent beampattern synthesis using non-linearly increasing frequency offsets," *IET Microwaves, Antennas & Propagation*, vol. 10, no. 8, pp. 880–884, 2016.

[17] Z. Wang, W.-Q. Wang, and H. Shao, "Range-azimuth decouple beamforming for frequency diverse array with Costas-sequence modulated frequency offsets," *EURASIP Journal on Advances in Signal Processing*, vol. 2016, p. 124, 2016.

[18] W. Khan and I. M. Qureshi, "Frequency diverse array radar with time-dependent frequency offset," *IEEE Antennas and Wireless Propagation Letters*, vol. 13, pp. 758–761, 2014.

[19] A. Yao, W. Wu, and D. Fang, "Solutions of time-invariant spatial focusing for multi-targets using time modulated frequency diverse antenna arrays," *IEEE Transactions on Antennas and Propagation*, vol. 65, no. 2, pp. 552–566, 2017.

[20] A. Yao, P. Rocca, W. Wu, A. Massa, and D. Fang, "Synthesis of time-modulated frequency diverse arrays for short-range multi-focusing," *IEEE Journal of Selected Topics in Signal Processing*, vol. 11, no. 2, pp. 282–294, 2017.

[21] A. Yao, W. Wu, and D. Fang, "Frequency diverse array antenna using time-modulated optimized frequency offset to obtain time-invariant spatial fine focusing beampattern," *IEEE Transactions on Antennas and Propagation*, vol. 64, no. 10, pp. 4434–4446, 2016.

[22] Z. Ahmad, Z. Shi, and C. Zhou, "Time-variant focusing range-angle dependent beampattern synthesis by uniform circular frequency diverse array radar," *IET Radar, Sonar & Navigation*, vol. 15, no. 1, pp. 62–74, 2021.

[23] W. Xu, L. Zhang, H. Bi, P. Huang, and W. Tan, "FDA beampattern synthesis with both nonuniform frequency offset and array spacing," *IEEE Antennas and Wireless Propagation Letters*, vol. 20, no. 12, pp. 2354–2358, 2021.

[24] Y. Liao, W. Wang, and Z. Zheng, "Frequency diverse array beampattern synthesis using symmetrical logarithmic frequency offsets for target indication," *IEEE Transactions on Antennas and Propagation*, vol. 67, no. 5, pp. 3505–3509, 2019.

[25] Z. Wang, Y. Song, T. Mu, and Z. Ahmad, "A short-range range-angle dependent beampattern synthesis by frequency diverse array," *IEEE Access*, vol. 6, pp. 22664–22669, 2018.

[26] A.D. Poularikas, *Handbook of formulas and tables for signal processing*, Boca Raton, FL: CRC Press, 1998.

[27] Z. Jaffri, Z. Ahmad, A. Kabir, and S. Bukhari, "A novel compact stair-shaped multiband fractal antenna for wireless communication systems," *Journal of Electrical Engineering*, vol. 72, no. 5, pp. 306–314, 2021.

[28] Z. Jaffri, Z. Ahmad, A. Kabir, and S. Bukhari, "A novel miniaturized Koch-Minkowski hybrid fractal antenna," *Microelectro -nics International*, vol. 39, no. 1, pp. 22–37, 2022.

[29] Z. Ahmad, Y. Song, and Q. Du, "Wideband DOA estimation based on incoherent signal subspace method," *COMPEL-The International Journal for Computation and Mathematics in Electrical and Electronic Engineering*, vol. 37, no. 3, pp. 1271–1289, 2018.

[30] N. Goel and K. Singh, "Analysis of Dirichlet, Generalized Hamming and Triangular window functions in the linear canonical transform domain," *Signal, Image and Video Processing*, vol. 7, no. 5, pp. 911–923, 2013.

Received 29 December 2021

Zeeshan Ahmad received the PhD degree in information and communication engineering from Nanjing University of Science and Technology, Nanjing, China, in 2018. He is currently working as an Assistant Professor with the School of Electronic and Information Engineering, Ningbo University of Technology, Ningbo, China. His research interests include array signal processing, frequency diverse array radars, direction-of-arrival estimation, adaptive beamforming, and wireless communications.

Zain ul Abidin Jaffri received the PhD degree in communication and information systems from Chongqing University, Chongqing, China, in 2018. He is currently working as an Associate Professor with the College of Physics and Electronic Information Engineering, Neijiang Normal University, Neijiang, China. His research interests include wireless sensor networks, antenna design and propagation, mobile and wireless communication networks, and advanced computer networks.

Shu-Di Bao received the BS degree from Ningbo University, Ningbo, China, in 1999, and the MS and PhD degrees from the Southeast University, Nanjing, China, in 2003 and 2007, respectively, all in communications and information systems. She is currently a Professor with the School of Electronic and Information Engineering, Ningbo University of Technology, Ningbo, China. Her research interests include information retrieval, security and fault tolerance, efficient communications for body sensor networks, and telemedicine systems.

Meng Chen received the Master's degree in computer application engineering from Zhejiang University of Technology, Hangzhou, China. He is currently an Associate Professor with the School of Electronic and Information Engineering, Ningbo University of Technology, Ningbo, China. His research interests include mobile health system security, biometrics, and information security.